Motions of Single Molecules and Proteins in Trehalose Glass

Erwen Mei, Jianyong Tang, Jane M. Vanderkooi, and Robin M. Hochstrasser*

Contribution from the Department of Chemistry and Department of Biochemistry and Biophysics, University of Pennsylvania, Philadelphia, Pennsylvania 19104

Received September 20, 2002 ; E-mail: hochstra@sas.upenn.edu.

Abstract: The fluorescence intensity−time records of individual metal-free porphyrin cytochrome-*c* and Zn porphyrin cytochrome-*c* molecules whose translational motions are restricted by encapsulation in trehalose are examined by single-molecule spectroscopy by means of a two-channel confocal microscope that records transient fluorescence signals in two orthogonal polarization directions. Large angular motions often occur on time scales ranging to many seconds. Measurements of the photobleaching time distributions indicate that the trehalose glass restricts the accessibilty of the fluorescent molecules to oxygen.

Introduction

Water is essential for life: dehydration generally inactivates proteins and enzymes. However, pollen, seeds, fungal spores, and a variety of microscopic animals can survive dehydration for decades and restore activity within minutes of rehydration.[1] The secret of the survival from anhydrobiosis of many organisms was found to be correlated with the presence of the disaccharide trehalose (α-D-glucopyranosyl-α-D-glucopyranoside). Trehalose is well-known for its ability to preserve life in cells, organisms, and biomolecules under conditions of high[2] and low temperature.[3,4] The mechanism by which trehalose exerts protection has been widely explored.[5−11] Spectroscopic studies indicated that trehalose may replace water molecules in forming hydrogen bonds to the surface of the protein and, hence, protect protein from dehydration.[12,13] Other studies have suggested that the trehalse glass exerts its bioprotection through the entrapped water molecules in the protein−trehalose mixture.[14,15] Trehalose can also prevent the loss of internal water molecules of protein.[7] The ability of the sugar to form a glass appears to be essential for its bioprotective properties.[16−18]

Trehalose forms viscous solutions and glasses at room temperature that have proved useful in studies of protein dynamics such as the kinetics of geminate recombination of carbon *monoxide* to myoglobin.[6,7] In another example, when bovine rhodopsin was suspended in trehalose−water glass films, it was possible to trap intermediates in the light-activation process, allowing for facile room-temperature investigations of the spectroscopic properties of rhodopsin's photointermediates.[19] These examples show that proteins can undergo function in trehalose although with considerably slowed rates.

Recent developments in single-molecule spectroscopy provide effective methods for studying structural and dynamical features of individual molecules interacting with their surroundings.[20−25] Such measurements yield direct information on the distributions of properties that exist in the equilibrium ensembles. We report here on the fluorescence polarization properties of single proteins in trehalose glasses. The results are expected to allow the characterization of the distribution of environments or cavities in which the proteins are confined and the range of physical properties exhibited by the proteins. A large number of single-molecule measurements can also be averaged to yield something approaching a bulk response whose underlying microscopic dynamics at equilibrium is known.

Materials and Methods

A. Samples. Trehalose (α,α-trehalose) purchased from Sigma Chem. Co. (St. Louis, MO) was directly used to prepare trehalose aqueous solutions. Zn Cyt-*c* and metal-free P Cyt-*c* were prepared from horse Cyt-*c* as previously described.[26] Solutions of rhodamine-6G (Rh6G),

(1) Crowe, F. H.; Crowe, L. *Annu. Rev. Physiol.* **1992**, *54*, 579−599.
(2) Bianchi, G.; Gamba, A.; Murelli, C.; Salamini, F.; Bartels, D. *Plant J.* **1991**, *3*, 355−359.
(3) Chen, Y.; Foote, R. H.; Brockett, C. C. *Cryobiology* **1993**, *30*, 423−431.
(4) Storey, K. B.; Baust, J. G.; Storey, J. M. *J. Comput. Physiol.* **1981**, *144*, 183−190.
(5) Woelders, H.; Matthijs, A.; Engel, B. *Cryobiology* **1997**, 93−105.
(6) Hagen, S. J.; Hofrichter, J.; Eaton, W. A. *J. Phys. Chem.* **1996**, *100*, 12008−12021.
(7) Sastry, G. M.; Agmon, N. *Biochemistry* **1997**, *36*, 7097−7108.
(8) Soren, B. E.; Serge, P. *J. Phys. Chem.* **2000**, *104*, 9301−9311.
(9) Bonincontro, A.; Bultrini, E.; Calandrini, V.; Cinelli, S.; Onori, G. *J. Phys. Chem. B* **2000**, *104*, 6889−6893.
(10) Singer, M. A.; Lindquist, S. *Mol. Cell* **1998**, *1*, 639−648.
(11) Schlichter, J.; Friedrich, L.; Herenyi, L.; Fidy, J. *Biophys. J.* **2000**, *80*, 2011−2017.
(12) Carpenter, J. F.; Crowe, J. H. *Biochemistry* **1989**, *28*, 3916−3922.
(13) Prestrelski, S. J.; Tedeschi, N.; Arakawa, T.; Carpenter, J. F. *Biophys. J.* **1993**, *65*, 661−671.
(14) Grazia, C.; Giovanni, C.; Lorenzo, C. *J. Chem. Phys.* **2002**, *117*, 9862−9866.
(15) Belton, P. S.; Gil, A. M. *Biopolymers* **1994**, *34*, 957−961.
(16) Green, J. L.; Angell, C. A. *J. Phys. Chem.* **1989**, *93*, 2880−2882.
(17) Miller, D. P.; Pablo, J. J. d.; Corti, H. R. *J. Phys. Chem.* **1999**, *103*, 10243−10249.

(18) Ding, S. P.; Fan, J.; Green, J. L.; Lu, Q.; Sanchez, E.; Angell, C. A. *J. Thermal Anal.* **1996**, *47*, 1391−1405.
(19) Sikora, S.; Little, A. S.; Dewey, T. G. *Biochemistry* **1994**, *33*, 4454−4459.
(20) Xie, X. S. *Acc. Chem. Res.* **1996**, *29*, 598−606.
(21) Mehta, A. D.; Rief, M.; Spudich, J. A.; Smith, D. A.; Simmons, R. M. *Science* **1999**, *283*, 1689−1695.
(22) Moerner, W. E.; Orrit, M. *Science* **1999**, *283*, 1670−1675.
(23) Weiss, S. *Science* **1999**, *283*, 1676−1683.
(24) Mei, E.; Bardo, A. M.; Collinson, M. M.; Higgins, D. A. *J. Phys. Chem.* **2000**, *104*, 9973−9980.
(25) Deschenes, L. A.; Bout, D. A. V. *Science* **2001**, *292*, 255−258.

P Cyt-*c*, and Zn Cyt-*c* at ca. 10^{-9} M contained 1% trehalose by weight. Thin films were prepared by spin casting 20 μL of the trehalose solution onto a microscope cover slip and drying in air. Common glass microscope cover slips were used when preparing thin films containing Rh6G, while quartz cover slips (ESCO Products) were used for thin films containing P Cyt-*c* and Zn Cyt-*c*. The glass cover slips were cleaned by sequential sonication in sodium hydroxide, sulfuric acid, and deionized water before being dried under N_2. Quartz cover slips were cleaned by soaking in freshly prepared nochromix−concentrated sulfuric acid solution overnight, followed by rinsing with deionized water and drying under N_2. Deionized water was used throughout all experiments. Denatured Zn Cyt-*c* in trehalose was prepared by spin casting with hot Zn Cyt-*c* solution (~90 °C). Some experiments were carried out on spin-coated samples in the absence of trehalose, where the molecules are directly attached to the glass surface.

The water content in the trehalose film was measured from the infrared spectra of the films using a Bruker IFS 66 Fourier transform IR instrument (Bruker, Brookline, MA). The molar ratio of trehalose/water was ascertained from the ratio of the trehalose CH stretch at 2940 cm^{-1} and the water HOH bending motion at 1650 cm^{-1}. In a film made in the same manner as used for the single molecule studies, the molar ratio of water to trehalose was 2 ± 0.2. Although this is comparable with the water of hydration in crystalline trehalose, we could find no evidence of crystallinity as judged from properties in polarized light, indicating that any crystals would need to be much smaller than the wavelength of visible light.

B. Instrumentation. The scanning confocal microscope, described previously,[27] uses a sample-scanning stage (Queensgate) with closed-loop X, Y feedback for accurate sample positioning and location of individual molecules. The stage was controlled by a modified Nanoscope E Controller (Digital Instruments). The sample and stage were mounted on an inverted, epi-illlumination microscope (Nikon, Diaphot 300). Circularly polarized 514.5 and 488 nm lines of an argon ion laser were used in separate experiments to excite the Rh6G, P Cyt-*c*, and Zn Cyt-*c*, respectively. The excitation power in each case was in the range 0.3−1 μW. A Nikon FLUOR ×40, 1.3 numerical aperture objective was used to produce a nearly diffraction-limited focus on the sample and to collect the fluorescence. Appropriate combinations of notch (Kaiser Optical), band-pass, long-pass, and dichroic filters (Chroma Technology) were used to spectrally isolate the signals.

Two single-photon-counting avalanche diodes detected the photons reflected and transmitted by a polarizing beam splitter, thereby isolating the fluorescence emitted by the molecules into orthogonal polarization directions, s and p, in the plane of the microscope. The p-polarized fluorescence image, obtained by raster scanning the sample pixel by pixel, was used to locate molecules. Once located, a single molecule fluorescence spot was centered in the laser focus, and signals were collected in the two orthogonal polarization directions. The detected signals were binned in 1 ms intervals. The fluorescence spectra of single molecules were obtained by means of a monochromator (Acton Research) equipped with a back-illumination liquid nitrogen cooled CCD camera (Princeton Instruments, Trenton, NJ).

C. Polarization Expectations. Molecules with a single fluorescent state, such as with Rh6G, and whose unit transition dipole for absorption and emission has colatitude $\theta \equiv \theta(t)$ and azimuth $\phi \equiv \phi(t)$ in the orthogonal laboratory coordinates (s, p, N) should exhibit the following fluorescence intensities for circularly polarized light excitation:

$$I_p(t) - I_s(t) = \eta(\theta) \sin^4 \theta \cos 2\phi$$

$$I_p(t) + I_s(t) = \eta(\theta) \sin^4 \theta = I(t) \qquad (1)$$

where $\eta(\theta)$ is the collection efficiency of the microscope objective.[28] The ratio of the difference and sum of the intensities (the *dichroism*) is $A(t) = \cos(2\phi)$. When there are two participating orthogonal transition dipole directions *x* and *y* in the molecular frame (as for Zn Cyt-*c*, a circular absorber and emitter with *x* and *y* the in-plane and *z* the out-of-plane axes) whose fluorescence intensities are dependent on the instantaneous polar angles of their dipoles, the dichroism is

$$A(t) = \frac{\eta(\theta_{xN})(s_x^2 - p_x^2) + \eta(\theta_{yN})(s_y^2 - p_y^2)}{\eta(\theta_{xN})(1 - N_x^2) + \eta(\theta_{yN})(1 - N_y^2)} \qquad (2)$$

where θ_{iN} is the angle between the transition dipole axis i and the N axis, and s_i, p_i, and N_i are the direction cosines of i onto s, p, and N. For the microscope objective used in this work,[28] $\eta(\theta) \approx \text{constant}(1 + \sin^2 \theta)$.

If, as is the case with P Cyt-*c*, the absorption and emission dipoles are perpendicular, then the *A* value is

$$A(t) = \frac{\cos^2 \theta - \sin^2 \theta \sin^2 \phi}{\cos^2 \theta + \sin^2 \theta \sin^2 \phi} \qquad (3)$$

where angles (θ, ϕ) now refer to the emission dipole orientation to the p-axis.

Results

The fluorescence spectra of single molecules of Rh6G, P Cyt-*c*, and Zn Cyt-*c* in trehalose (not shown) were indisinguishable from those in bulk water solution. The P Cyt-*c* and Rh6G molecules are linear oscillators for which the fluorescence and absorbance steps each involve a single transition dipole. On the other hand, for bulk samples of Zn Cyt-*c* in trehalose the conventional fluorescence anisotropy[29] was measured to be 0.1 ± 0.01, confirming that it behaves like a circular oscillator on average. Figures 1−3 present some typical intensity−time records for Rh6G, P Cyt-*c*, and Zn Cyt-*c* molecules in trehalose. In each example the top record shows some typical motions, and the last record shows molecules that are relatively fixed in space. If the emitting transition dipoles were fixed in space, these records should display a significant p-signal for all observation times because of the bias in the choice of molecules from the image. Indeed a few molecules behaved in this manner in trehalose: 6.4% of a total of 171 Rh6G molecules and ~1.7% and ~14% of 159 folded molecules and 222 unfolded molecules of Zn Cyt-*c*. Otherwise the records often showed signals that alternated between the two orthogonal polarization directions. We have found no evidence that the molecular reorientations are in some way light induced. However it has not been possible to eliminate the occurrence of such processes. On the other hand, a number of observations suggest that the reported variations in *A* are not light induced. (1) Any light-induced process would need to be applicable to only certain molecules, since some molecules show very little motion. (2) A few molecules showed changes in orientation after the laser had been blocked for about 10 s. In some examples there was no change in *A*; in others there were significant changes in *A*. (3) In many of the intensity−time records there occur dark states that have no detectable emission, which must correspond to molecules converted into forms that have very low fluorescence yields in the

(26) Vanderkooi, J. M.; Adar, F.; Erecinska, M. *Eur. J. Biochem.* **1976**, *64*, 381−387.
(27) Bopp, M. A.; Sytnik, A.; Howard, T. D.; Cogdell, R. J.; Hochstrasser, R. M. *Proc. Natl. Acad. Sci. U.S.A.* **1999**, *96*, 11271−11276.
(28) Bopp, M. A.; Jia, Y.; Haran, G.; Morlino, E. A.; Hochstrasser, R. M. *Appl. Phys. Lett.* **1998**, *73*, 7−9.
(29) Dixit, B. B. S. N.; Waring, A.; Wells, K.; Wong, P.; Woodrow, G. V., III; Vanderkooi, J. M. *Eur. J. Biochem.* **1982**, *126*, 1−9.
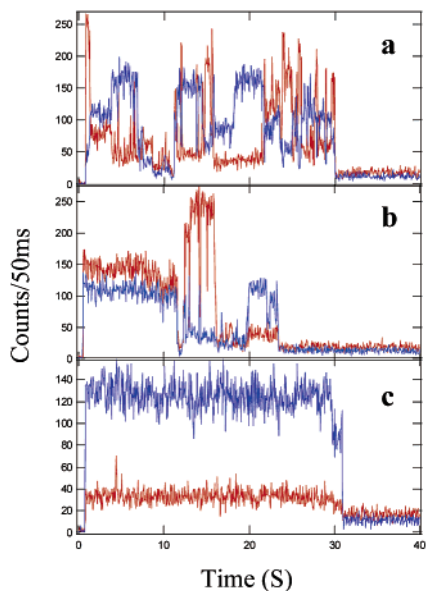
Figure 1. Representative time-dependent records of transient fluorescence intensities of single Rh6G molecules in trehalose detected in two orthogonal polarization directions.

Figure 2. Representative time-dependent records of transient fluorescence intensities of single P Cyt-*c* molecules in trehalose detected in two orthogonal polarization directions.

Figure 3. Representative time-dependent records of transient fluorescence intensities of single Zn Cyt-*c* molecules in trehalose detected in two orthogonal polarization directions.

detected region or no absorption. We found that the dichroism frequently had changed when the fluorescence signal reappeared, indicating that motion continued during the nonemission period. If light-induced motion required an electronically excited state to initiate it, then when that electronic state is no longer formed or has its emission lifetime severely reduced by quenching, either of which may occur in the dark state, we would expect that light-induced motions would be diminished or quenched. Of course other pathways to motion, perhaps through vibrational excitations, might be opened up in the quenched state. However at present we do not know the extent to which dark states absorb the excitation light. Moreover, the dark states are not observed to exhibit any significant increase in angular motion. The intensity time records for the single molecules exhibit very little systematic behavior that repeats from record to record, with only a few qualitative properties being typical of the complete data set. The records often show significant, slow (ca. 5 s) variations of the signal during which the signal polarization alternates around a relatively well-defined mean value. The photobleaching characteristics are shown in Figures 4 and 5. Data taken for molecules on a glass surface are shown for comparison with those in trehalose in Figure 4a and c. The dye molecules in trehalose emit on average 3.8 times more total photons than do their counterparts on glass. Fluorescence intensity–time records were also used to calculate the total time prior to permanent photobleaching (Δt) under continuous illumination using a fixed source intensity. The survival times of P Cyt-*c* and Zn Cyt-*c* under the same illumination conditions are shown in Figure 5a and b. Many more P Cyt-*c* molecules live for times exceeding 20 s.

Single-Molecule Characteristics. The results show that the distribution of parameters needed to describe the behavior of single molecules is very broad, indicative of a very heterogeneous collection of trehalose fluorescent centers. The varied behavior of the dichroism of single molecules shows that the motions are not simply due to unrestricted rotational diffusion. It is apparent from the polarization data that there are angular motions of the transitio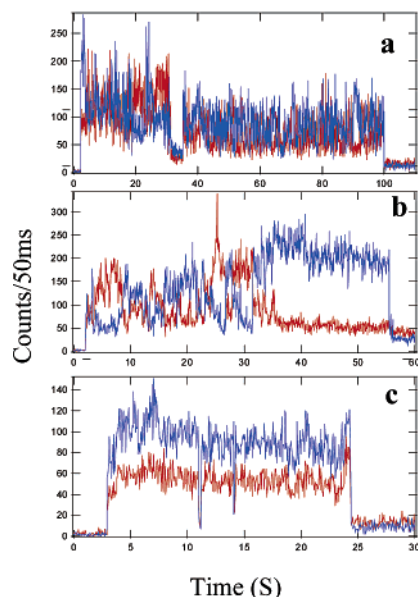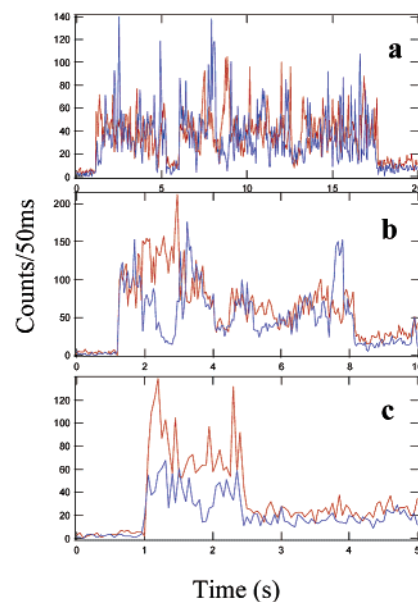n dipoles, but these motions are quite restricted. There is a range of dichroism properties: some single-molecule records show a fairly constant dichroism, while others show rapid changes, and still others show constant values followed by regions where the dichroism fluctuates, while others show fluctuations of dichroism on a range of time scales. The results imply that the angular motion properties of a center will often change during the single-molecule fluorescence recording. Because of this heterogeneity, we do not attempt to find a description that encompasses all the single-molecule behavior. Instead we present histograms whose purpose is to document the extent of the heterogeneity and to investigate the statistical significance of any differences in behavior for the three molecular structures studied. The contribution from molecular reorientation to the fluctuations in the intensity–time records varies from molecule to molecule, but the signals also contain
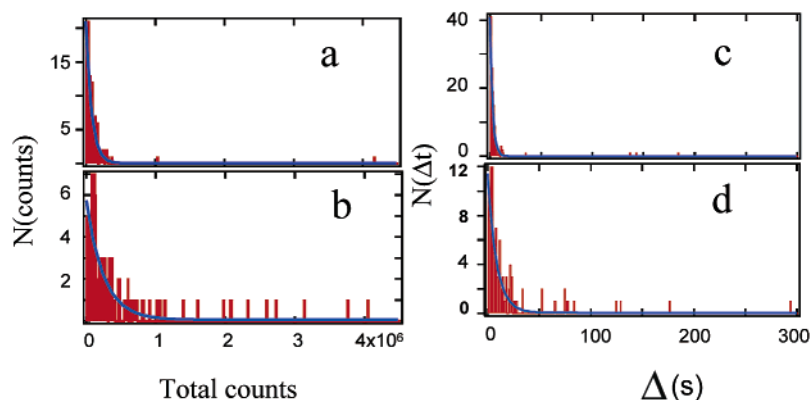
Figure 4. (a and b) Histograms of the total photons emitted by single Rh6G molecules immobilized on a glass surface and entrapped in trehalose, respectively. (c and d) Histograms of the survival times for the same set of Rh6G molecules on a glass surface and in trehalose.
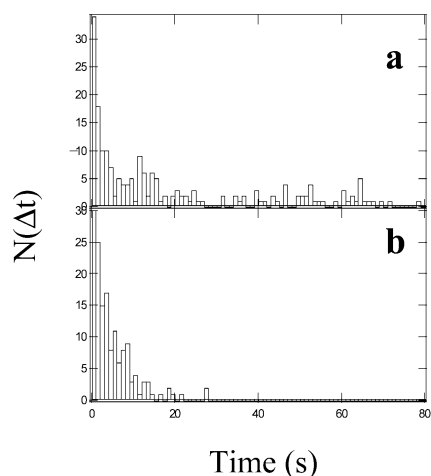

Figure 5. Histograms of the survival times for single P Cyt-*c* (a) and Zn Cyt-*c* (b) molecules entrapped in trehalose.

Figure 6. Histogram of the standard deviation of the dichroism, $\sqrt{\langle A^2 \rangle - \langle A \rangle^2}$, of single P Cyt-*c* and Zn Cyt-*c* molecules entrapped in trehalose. (a) P Cyt-*c* calculated by using full length of trajectories; (b) Zn Cyt-*c* and (c) P Cyt-*c* calculated by using partial length of records as discussed in the text.

significant Poisson noise that obscures the visualization of some of the motions. The common way to quantitatively evaluate the effect of noise on single-molecule data is to generate a distribution of parameters by using Poisson variables (usually experimental noise, which has a fixed mean).[30,31] But in our experiments, dichroism varies from molecule to molecule in a wide range. One can see clearly the noise contribution from the single-molecule trajectories. For example, in Figures 1c and 2c, the mean value of *A* across the whole time record is nonzero and the distribution of *A* values around the mean follows Poisson statistics. On the other hand, the molecules shown in Figures 1a and b and 2b are clearly moving and the distribution of *A* around the mean is much wider than the Poisson distribution. The example in Figure 3a indicates a mean of *A* that is close to zero ($I_p \cong I_s$) and the angular fluctuations are more obscured by the Poisson noise. Therefore it is clear that the distributions of *A*, δ*A*, and φ (Figures 6−8) are not determined by shot noise fluctuations. Shot noise did play a role when we tried to analyze the dichroism fluctuations seen on the 10 ms or less time scales. Figures 2a and 3a show typical examples of such variations. These fast fluctuations appear to be restricted motions, and although they were quite common, they were not fully characterized. To plot these histograms, we have rebinned the data to a bin interval of 50 ms, which eliminates the possibility of
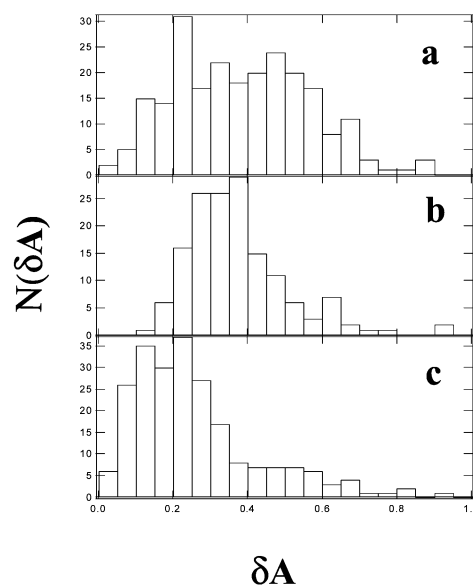
analyzing motions any faster than this. First we plotted the histogram of the fluctuation in the dichroism defined for each molecule as $\delta A = \sqrt{\langle A^2(t) \rangle - \langle A(t) \rangle^2}$, where the average is over the intensity−time record with *t* in increments of 50 ms. These results, shown in Figure 6a and b for P Cyt-*c* and Zn Cyt-*c*, respectively, provide a very qualitative overview of the dichroism variations. Of course the variance in the dichroism should depend on the length of the intensity−time record if there are motions that are occurring on shorter time scales than the records. Indeed this is the case, as can be seen from Figure 6c, which plots the δ*A* histogram for P Cyt-*c* using only portions of the records. In Figure 6c the lengths of the portions for analysis were chosen from a Gaussian distribution having the mean value and variance of the lengths that were obtained experimentally from the much shorter Zn Cyt-*c* records. It is seen that the variance histograms for Rh6G, P Cyt-*c*, and Zn Cyt-*c* are much more similar when the record length distributions are chosen to have the same variance.

(30) Deniz, A. A.; Dahan, M.; Grunwell, J. R.; Ha, T.; Faulhaber, A. E.; Chemla, D. S.; Weiss, S.; Schultz, P. G. *Proc. Natl. Acad. Sci. U.S.A.* **1999**, *96*, 3670−3675.

(31) Sophie, B.; J. G., P. E.; Atsushi, M.; W. E., M. *J. Phys. Chem. B* **2000**, *104*, 3676−3682.
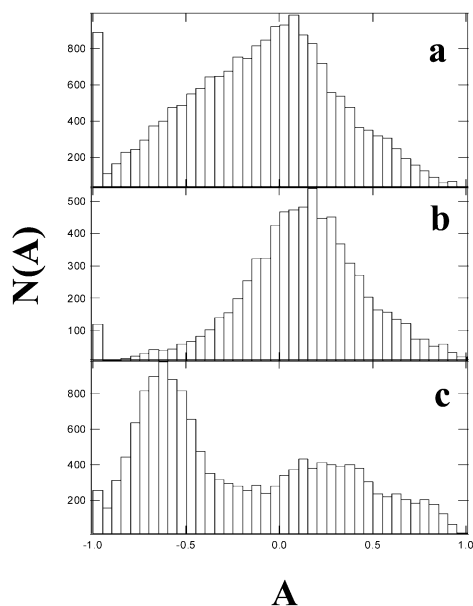
Figure 7. Distribution of the dichroism, A, of single molecules entrapped in trehalose: (a) P Cyt-c, (b) Zn Cyt-c, and (c) Rh6G.
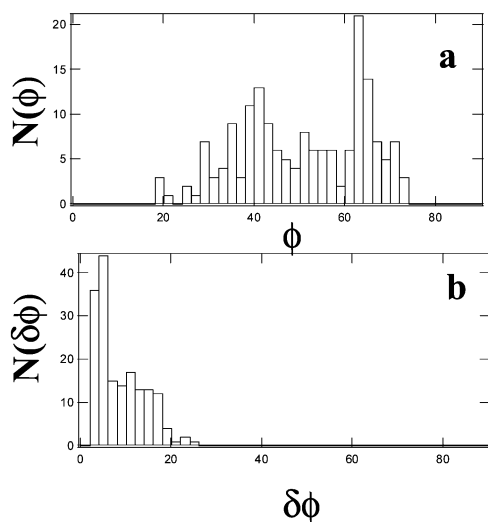

Figure 8. Distributions of (a) the azimuthal angle ϕ and (b) the standard deviation of ϕ, both calculated from records of single Rh6G molecules in trehalose.

Equation 1 predicts that if a linear dipole oscillator samples all possible orientations with equal probability during the total observation period of the record, we should find its A value continuously distributed between -1 and 1, with peaks in the distribution at 1 and -1. For a circulator oscillator the distribution of A values should peak at 1, 0, and -1 with probabilities 1:2:1. However the dynamic range of the experiment is such that the largest measurable ratio of I_p/I_s or I_s/I_p is ca. 5. This implies that the peaks in the distribution of A should be at ca. ±0.63 instead of ±1. Figure 7 shows the distributions of A computed over the first 5 s of each molecule's record with a binning width of 50 ms. If the molecules were fixed, the distribution would peak between $A = 0$ and $A = 1$ because the choice of the molecule in the first place was determined by its visibility in p-polarization. Other molecules also show peaks between $A = 0$ and $A = -1$ indicative of motion. When A reaches a value near to zero, the shot noise causes the s and p signals to alternate in intensity as if there were fluctuations in

A about zero that have the appearance of very fast (tens of ms) restricted rotational motions. Using eq 1 we can also compute the variance in the angle ϕ for the case of the linear dipole oscillator Rh6G, for which the results are shown in Figure 8. The low dynamic range of the experiment effectively eliminates the contributions from angles too close to 0° and 90°. For the purpose of this paper these fluctuations are averaged over by enlarging the binning width.

In the experiment each photon collected arises from a particular choice of both the excitation and emission polarization; therefore, the autocorrelation functions of A and I are quite different from those obtained from conventional bulk fluorescence polarization measurements. If there were a small step rotational diffusion, these correlation functions, based on the definitions in eqs 1–3, are readily computed from the conditional probabilities for diffusing objects.[32] For a spherical diffuser (diffusion coefficient D) direct integration yields a power series in which the nth term is $a_n[\exp\{-Dt\}]^{n(n+1)}$ where n is an even integer. The ratio of the amplitudes a_2/a_4 is calculated to be 0.12. Neither the amplitudes nor the time constants predicted by this model are in agreement with the experiments on single molecules or the averages of the data for many molecules: the observed angular motions occurring during the limited existence time of the intensity time records incorporate large repeated angular jumps characteristic of restricted motions. It is quite clear from the records that the system is not close to being ergodic; therefore we are loathe to present correlation functions.

Survival Times. The total photons emitted by single molecules give important information about the nature and formation of the trehalose glass. As noted earlier, the results in Figure 4a and b show that the total number of photons emitted (on average) by Rh 6G single molecules is significantly greater in trehalose than on a glass surface. Also the average survival time of the molecules in trehalose film is about 3- to 4-fold larger than on glass. Possible explanations for the increase in total emitted photons include an increase in the fluorescence quantum yield of the dye or an increase in dye stability, as manifested by a reduction in the rate of photobleaching. However the average emission rates are similar in trehalose and on glass under the same continuous illumination conditions, indicating that the increase in total number of photons emitted results from the increase in survival time. Therefore these increases result primarily from increased photostability, consistent with other work on entrapped probes.[24,33] The increased dye stability observed in the trehalose film could result in a decrease in the intersystem crossing rate, a decrease in triplet lifetime, and/or a reduction in the oxygen permeability/mobility, but the nearly equal average photon emission rates observed for Rh6G under different conditions suggest that the reduction in the oxygen permeability/mobility is the essential stabilizing factor.

Angular Motions. The angular motions are likely to be occurring for solvent/solute cavities having a very wide range of sizes and hydrogen-bonded network structures but are nevertheless tailored to encapsulate molecules of different sizes. However the cavities can change their properties with time due to reconstruction of the trehalose structures in the glass. Such

(32) Berne, B.; Pecora, R. *Dynamic Light Scattering*; Wiley Interscience: New York, 1976.
(33) Negishi, N.; Fujino, M.; Yamashita, H.; Fox, M. A.; Anpo, M. *Langmuir* **1994**, *10*, 1772–1776.

changes in the glass structure will alter the time scales of the rotational fluctuations of the encapsulated molecule. The extraordinary heterogeneity of our results suggests that it is reconstruction of the trehalose glass/protein regions that is responsible for the protein dichroism changes that evidence the overall motions. Our data cannot yet be fitted to a simple model in which the trehalose forms a relatively narrow distribution of cavities within which the proteins undergo restricted rotation. The distribution of cavity properties would be required to be considerably wider than our data set. So some reconstruction of trehalose in the neighborhood of the dissolved protein regions is suggested. In aqueous solution, it is known that a hydration shell, consisting of several layers of water, surrounds protein molecules.[34–36] During the formation of the trehalose film, protein molecules along with some of their hydration should be co-encapsulated by the trehalose glass. It is usually supposed that the sugar replaces the water molecules in forming hydrogen bonds to the surface of the protein.[12] According to our analysis, there are about two water molecules for each trehalose molecule in the glass. So the experiment is being carried out far from the glass transition.[18] The surface area of a cavity confining Cyt-*c* requires a minimum of ca. 40 trehalose molecules. The importance of water molecules in determining the properties of proteins in trehalose has been discussed before. For example, it was suggested that trehalose prevents the escape of some vital internal water molecules from encapsulated myoglobin, thus preserving the internal lability of the protein.[7] Measurements of the dehydration process of trehalose glasses with encapsulated carbonmonoxy-myoglobin indicated that a microcrystallization process takes place during dehydration;[37] moreover, the crystal-

linity is maintained unless the dry samples are humidified. The low oxygen permeability/mobility in our trehalose preparations is evident from the results of Figure 4, which also indicate that the glass is rigid. The reconstruction process might be related to the dynamics of incorporated water. The method of preparing the sample may also be quite critical for a material like trehalose, which could quite readily crystallize during a spin-coating process. These suggestions will be tested by studies at different temperatures, methods of preparing the glasses, and their water contents and will form the basis of future work.

Conclusions

A two-channel polarization confocal microscope has been used for investigating the reorientations of single molecules and proteins in trehalose glass. Information about the formation and the nature of trehalose glass as well as the interactions between the dopant and its surrounding trehalose microenvironments has been obtained by analyzing the photostability and orientational motions of proteins and dye molecules in trehalose. The entrapped molecules are approximately 3.4 times more stable than their counterparts on glass surfaces, which evidences the low oxygen permeability/mobility in trehalose glass. Significant angular motions of the transition dipoles of single Rh6G, P Cyt-*c*, and Zn Cyt-*c* molecules encapsulated in trehalose have been observed on time scales ranging into the many seconds regime. Experimental results indicate an extremely heterogeneous behavior, which is not readily interpreted as restricted rotors in a relatively narrow distribution of well-defined trehalose cavities.

JA021197T

(34) Tarek, M.; Tobias, D. J. *Biophys. J.* **2000**, *79*, 3244–3257.
(35) Finney, J. L. *Faraday Discuss.* **1996**, *103*, 1–18.
(36) Luzar, A. *Faraday Discuss*. **1996**, *103*, 29–40.
(37) Librizzi, F.; Vitrano, E.; Cordone, L. *Biophys. J.* **1999**, *76*, 2727–2734.